COMPDYN 2021
8th ECCOMAS Thematic Conference on
Computational Methods in Structural Dynamics and Earthquake Engineering
M. Papadrakakis, M. Fragiadakis (eds.)
Streamed from Athens, Greece, 28-30 June 2021

EXPERIMENTAL STUDY ON THE IN-PLANE RESPONSE OF ADOBE MASONRY WALLETS STRENGTHENED WITH TEXTILE REINFORCED MATRIX SYSTEMS

Paolino Cassese[1], Luigi Fenu[2], Domenico Asprone[3], Antonio Occhiuzzi[4,5] and Fulvio Parisi[3]

[1] National Research Council (CNR), Construction Technologies Institute (ITC)
c/o Polo Tecnologico di San Giovanni a Teduccio, Naples, Italy - paolino.cassese@itc.cnr.it

[2] University of Cagliari, Department of Civil Engineering, Environment Engineering and Architecture
Via Marengo 2, Cagliari, Italy - lfenu@unica.it

[3] University of Naples Federico II, Department of Structures for Engineering and Architecture
Via Claudio 21, Naples, Italy - d.asprone@unina.it, fulvio.parisi@unina.it

[4] National Research Council (CNR), Construction Technologies Institute (ITC)
Viale Lombardia, 49, San Giuliano Milanese, Italy - occhiuzzi@itc.cnr.it

[5] University Parthenope, Department of Engineering
Centro Direzionale Isola C4, 80143 Naples, Italy - antonio.occhiuzzi@uniparthenope.it

Abstract

Seismic strengthening of existing adobe masonry (AM) buildings has been recognized as a critical issue due to the dramatic consequences of recent seismic events occurred especially in developing countries, where a great part of the population lives in those constructions. Previous studies investigated the effectiveness of different retrofitting techniques by means of experimental programs consisting of either dynamic or static tests on reduced- or full-scale specimens, representing partial or complete AM dwellings. In this study, the output of diagonal compression tests on adobe masonry panels before and after external strengthening are presented. Three series of specimens were tested, namely, unreinforced and strengthened wallets with textile reinforced matrix (TRM) systems made of either hemp or glass meshes. Those tests benefitted from the characterization of the mud mortar that was used for both masonry joints and matrix, representing typical characteristics of existing Italian AM buildings. Main testing outcomes obtained for the AM wallets, particularly in terms of observed damage and response curves, are presented and discussed. In the end, the effectiveness of the applied TRM systems in the improvement of shear strength and ductility capacity is assessed.

Keywords: Adobe masonry; Experimental tests; Textile reinforced matrix; Shear strength; Ductility; Hemp fibres; Glass fibres; Mud mortar.

1 INTRODUCTION

Since ancient times, a large part of civil and historical buildings were realized in adobe masonry (AM), representing nowadays one of the most widespread structural typology in the world, especially in developing countries [1-4]. Furthermore, such constructions are not engineered and the recent seismic events showed their vulnerability with dramatic consequences for residents [5, 6].

In the recent past, seismic strengthening of existing AM buildings has been recognized as a paramount issue. Indeed, a number of researchers investigated the effectiveness of different retrofitting techniques via experimental testing. Several studies dealt with dynamic testing on reduced-scale specimens representative of AM dwellings, strengthened by means of mesh-reinforcement embedded in mud-mortar [5, 7-10], horizontal low-cost post-tensioning straps [11-13], systems of internal/external interconnected grids [14], combined mud-grout injection of cracks and external mesh-reinforcement [15-16]. Such techniques proved to be very promising in reducing seismic vulnerability of AM constructions, even though more detailed and comprehensive assessments should be carried out.

Few experimental studies focused on the external strengthening of real-scale AM wallets, most of which based on mesh-reinforced plasters. Specifically, cyclic tests on real-scale AM walls were described in [17]. The specimens were firstly tested in the as-built configuration, then, hydraulic lime grout was injected in the cracks and synthetic mesh incorporated in the plaster was applied. The strengthening system restored the initial stiffness and improved both lateral strength and ductility. Similar findings were presented in [18]. Finally, Turanli and Saritas [19] performed diagonal compression tests on AM specimens externally strengthened with plaster reinforcement mesh placed along mortar bed joints. Despite the increased strength and energy absorption capacity, such solution appeared to be unfeasible for strengthening existing AM buildings.

Earthen dwellings can also be found in Italy, especially in Sardinia island, where such structural typology was largely adopted until mid-last century and, currently, represents a considerable part of existing buildings [20]. Sardinian AM constructions were generally realized with adobe blocks reinforced with straw fibres, according to practice rules without any seismic design [21]. Within the framework of a comprehensive research program on seismic assessment and retrofitting of existing Sardinian AM dwellings [6, 21-24], the present study deals with the results of diagonal compression tests on AM wallets. Specifically, three series of specimens were tested, namely: unreinforced and strengthened with two different textile reinforced matrix (TRM) systems, made of hemp and glass meshes, respectively. The hemp-based TRM system (HTRM hereinafter) was composed of natural and sustainable hemp fibres, which however were characterized by considerable variability in mechanical properties due to production process. Conversely, the glass-based TRM system (GTRM) was produced using a commercial glass-fibre mesh, which is usually adopted for strengthening of other traditional masonry structures. Both hemp and glass textiles were embedded in the same mud mortar detected in masonry joints of existing Italian AM buildings.

The following sections describe the experimental campaign, presenting its main outcomes in terms of observed damage, response curves, and effectiveness of the applied TRM systems in the improvement of shear strength and ductility capacity for the AM wallets.

2 EXPERIMENTAL CAMPAIGN

Diagonal compression tests were performed on 21 specimens equally divided into three series: unreinforced AM wallets (URM series); HTRM-strengthened AM wallets (HTRM series); and G-TRM-strengthened AM wallets (GTRM series). The adopted on-site

experimental set-up typology, suggested by relevant technical codes for existing masonry [25-27], allowed avoiding the handling of specimens with reduced disturbance before testing.

2.1 Materials and specimens

AM blocks used for specimens' construction were obtained by pressing a mixture of soil, water and straw fibres into moulds with grooved internal surfaces, whereas mud mortar with same composition of AM blocks (except straw fibres) was used for both masonry joints and TRM matrix, according to traditional Sardinian practice [20]. The experimental characterization of masonry was carried out in [21, 23].

The adopted hemp textile was a bidirectional grid with mesh of 20×20 mm^2 and thickness equal to 4 mm, which was made of three twisted yarns impregnated through epoxy resin according to 70% fraction by volume, in order to preserve its durability. Tensile strength per unit length of reinforcement was obtained by testing and Young's modulus was deducted given the value of volumetric resin fraction. More details can be found in [28]. A commercial glass fibre reinforced biaxial grid was used for strengthening of GTRM specimens. The mesh was equal to 25×25 mm^2, with yarns of thickness equal to 3 mm and 2 mm along weft and warp directions, respectively. The grid was coated with an acrylic polymer mixture. Material properties were provided by the supplier.

Main mechanical properties of the materials used for test specimens are summarized in Table 1. In detail, the mean value and coefficient of variation (*CoV*) are provided for compressive strength (f_c), tensile strength (f_t) and Young's modulus (E). It is noticed that CoV is not reported for material properties of glass fibre grid, given the lack of data by the supplier, and tensile strength of the hemp grid is given as force per unit length, due to diameter variability of the cord.

Property	AM block	Mortar	Hemp grid	Glass grid
f_c (N/mm^2)	1.08	0.50	-	-
CoV	36%	14%	-	-
f_t (N/mm^2)	0.56	0.45	20*	1276
CoV	36%	20%	15%	n.a.
E (N/mm^2)	143	49	6500 - 7000	72000
CoV	40%	47%	n.a.	n.a.

* *Tensile strength in terms of kN/mm*
n.a.: not available data

Table 1: Mechanical properties of the adopted materials.

Adobe blocks used for construction of AM wallets were approximately 200×400×100 mm^3 in size. Mud mortar joints were 10 mm thick. Two-leave AM specimens were fabricated with running bond configuration, reaching a size of 410×1230×1230 mm^3. For both HTRM and GTRM series, the TRM was applied on both sides of the wallets. First, the wallet was externally hydrated. Then, a 10-mm-thick layer of mud mortar was applied. When mortar was still fresh, the textile was installed. Finally, a covering layer of mortar was applied until a total 25 mm thickness was reached. Special attention was paid to hemp-fibre grids for which an ad-hoc, on-site fabrication process was implemented. Hemp meshes were realized by means of a proper wooden frame on which nails were placed with 20 mm spacing. Yarns were arranged along both warp and weft directions by using the nails as guide, then were impregnated of res-

in. Finally, square textiles with same specimens' dimensions were obtained by cutting. Figures 1 and 2 show a schematic view of specimens and details on fabrication of hemp mesh.

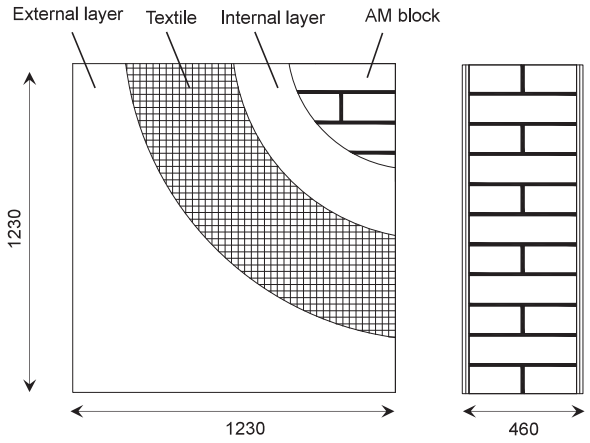

Figure 1: Layout of reinforced specimen.

Figure 2: Detail of the on-site fabrication of hemp mesh.

2.2 Testing setup and procedure

In order to reduce disturbance on specimens, the diagonal compression tests were performed directly in the manufacturing site by means of the movable system depicted in Figure 3. Specifically, the diagonal load was applied by reaction of a closed system with respect to the elongation of a hydraulic jack. Steel shoes were installed at both specimen's corners in order to distribute compressive stresses. Between such shoes and the specimen, a proper filling with shrinkage-free mortar was realized. All specimens were erected on rigid blocks. Foam sheets with low density were interposed between AM wallets and support-block, with the aim to avoid potential friction. After the installation, the loading system was self-supporting.

Diagonal compression load was applied with displacement control at 0.01 mm/s rate until failure was observed. The installed monitoring system was able to record diagonal displacements and load. In addition, four linear variable differential transformers (LVDTs) were arranged on both external surfaces of the wallet according to the typical X configuration, as shown in Figure 3. The gauge length was equal to 400 mm.

The average shear stress (τ) was derived from recorded load (F) by applying the formulation suggested by the ASTM E519-15 [29] standard (ASTM hereinafter), which is based on pure shear assumption as given in Eq. (1) in which A represents the cross-section area of the specimen (i.e., length × thickness). The average shear strain (γ) on each side of the specimen

was obtained as the sum of the axial strains derived from LVDT displacement recordings along and perpendicular to the loading direction, respectively, as reported in Eq. (2).

$$\tau = 0.707\frac{F}{A} \tag{1}$$

$$\gamma = \varepsilon_x + \varepsilon_y \tag{2}$$

Figure 3: Picture of the experimental set-up.

3 MECHANICAL RESPONSE AND FAILURE MODE

Shear stress versus shear strain (τ-γ) curves for series URM, HTRM and GTRM, along with crack patterns at failure, are depicted in Figure 4. In order to discuss the obtained results, for each test main mechanical parameters of the wallet were defined: the peak shear stress (τ_p), the elastic limit shear strain (γ_{cr}) corresponding to a shear stress equal to $0.7\,\tau_p$, the shear strain at failure (γ_u), the latter assumed as associated to a strength drop of $0.2\,\tau_p$ beyond the peak. Accordingly, the ductility capacity (μ) of the wallet was the ratio of ultimate to elastic shear strain values, as reported in Eq. (3). Such parameters are summarized in Table 2 in terms of mean and CoV for each specimen series.

$$\mu = \frac{\gamma_u}{\gamma_{cr}} \tag{3}$$

By observing Figure 4, all the specimens presented a mechanical response characterized by a first linear elastic branch up to first cracking, then a nonlinear curve up to peak stress and finally a softening until failure was observed. The recorded response was globally affected by high dispersion in displacement and force, especially in the post-peak range.

UMR specimens were characterized by shear strength (τ_p) equal to 0.107 MPa on average with small dispersion (CoV = 7%). Conversely, ductility capacity (μ) resulted highly dispersed, with CoV = 41% and a mean value of 17.1. Unreinforced wallets showed similar damage patterns at failure. Large stair-stepping diagonal cracks were observed on the specimens, partially developed in joints and bricks. Shear failure occurred, resulting in quasi-brittle post-peak response.

Property	URM	GTRM	HTRM
τ_p (N/mm^2)	0.107	0.120	0.134
CoV	7%	14%	13%
γ_{cr} (-)	0.08	0.06	0.13
CoV	15%	20%	23%
γ_u (-)	1.37	2.38	7.57
CoV	52%	23%	13%
μ (-)	17.1	38.2	61.4
CoV	41%	19%	22%

Table 2: Experimental results of diagonal compression tests.

As expected, a higher shear strength was found for GTRM specimens, namely τ_p = 0.120 MPa on average, in spite of a larger scatter (CoV = 14%). Generally, a more gradual post-peak softening was observed with respect to the unreinforced specimens, resulting in considerably increased ductility capacity, the mean value of which was 38.2. Failure modes were characterized by debonding of reinforcing grids after diagonal cracking onset, due to reduced mechanical compatibility of glass grid with respect to mud matrix.

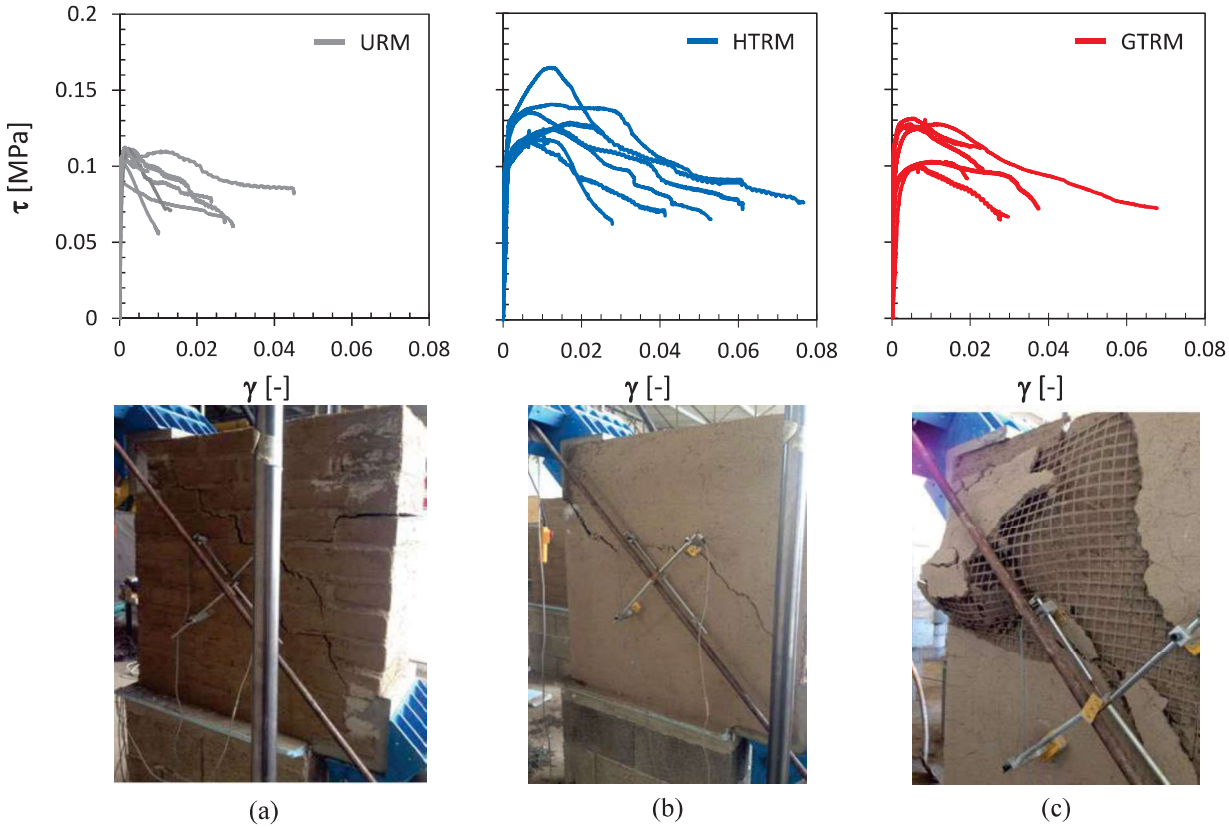

Figure 4: Experimental τ-γ curves and observed damage at the end of tests: (a) URM specimens; (b) HTRM specimens; (c) GTRM specimens.

No premature debonding occurred in the case of HTRM-strengthened wallets. The observed diagonal cracks followed the same profile of the inner unreinforced specimen; therefore, the imposed deformation was transferred to the TRM system up to global failure was

reached. HTRM-strengthened specimens showed a distinct hardening behaviour due to TRM up to peak strength, followed by a gradual strength degradation up to failure. The peak stress (τ_p) was equal to 0.134 MPa. Also in this case, significant scatter was recorded. Very high ductility capacity was obtained on average (μ = 61.4) with CoV = 22%.

4 STATISTICAL CONSTITUTIVE CURVES

Experimental testing confirmed a significant dispersion in the mechanical response of AM specimens. Specifically, high scattered values were recorded in terms of shear strain over all specimen series (i.e., URM, GTRM, HTRM). Regarding shear strength, considerably lower dispersion was observed with respect to strain, particularly in the case of URM specimens. With the aim of assessing the influence of such variability on TRM strengthening efficiency, a statistical analysis of the experimental results was carried out. Based on the assumption of normal distribution of the shear stress (considered as random variable) conditioned upon shear strain, τ-γ curves of the 16th, 50th (median) and 84th percentiles of conditional shear stresses were derived for each specimen series. Such curves are compared to each other in Figure 5. It is noted that diagrams are plotted up to 20% post-peak strength drop, which was assumed as ultimate limit state.

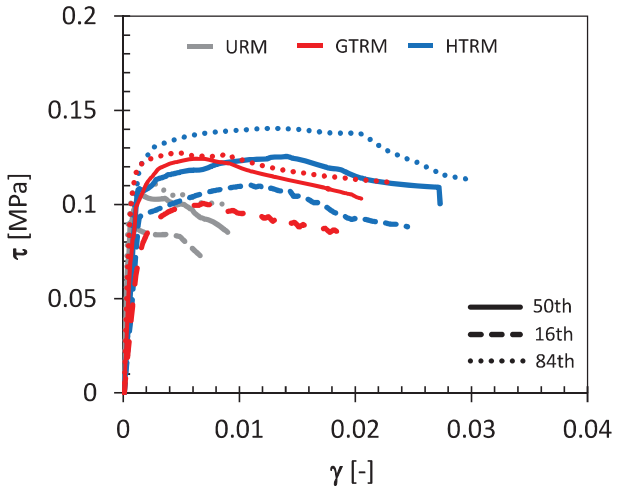

Figure 5: Statistical response curves corresponding to 16th, 50th and 84th percentiles of shear stresses.

Given the shear strain, the stress scatter (S) was computed as ratio of the difference between 84th and 16th values to the median value. Accordingly, similar scatter values were derived for URM and GTRM specimens, equal to 26% and 25%, on average, respectively. Conversely, a larger S-value was obtained for wallets strengthened by means of HTRM system (S = 39%). Such result was partially expected because of the higher variability in hemp grid production process, as opposed to commercial glass-grid for which stringent quality-control protocols are implemented during manufacturing [30]. By observing the statistical τ-γ curves, some general trend can be extrapolated regarding the efficiency of the two considered TRM strengthening systems. Response curves of URM specimens were characterized by negligible hardening, with peak strength reached in the elastic phase and a subsequent sudden drop in strength, resulting in a fragile failure mode. On the contrary, τ-γ diagrams of HTRM and TTRM series show a large hardening phase with gradual softening, representative of a more ductile failure. Therefore, in general, both TRM ensured considerable improvement of shear capacity, although the HTRM solution appeared more effective. In fact, on average, the increase of shear strength (e_τ, computed as ratio of the strengthened to unstrengthened peak

stress) in this latter case was equal to 1.31, whereas the mean increasing ductility factor (e_μ, defined as ratio of the strengthened to unstrengthened ductility capacities) was 3.60. By contrast, in the case of GTRM system, mean values of e_τ and e_μ were equal to 1.12 and 2.20, respectively. Average values of stress scatter (S) and efficiency factors (e_τ and e_μ) are summarized in Table 3.

Property	URM	GTRM	HTRM
S (%)	26	25	39
e_τ (-)	-	1.12	2.20
e_μ (-)	-	1.30	3.60

Table 3: Stress scatter and efficiency factors.

5 CONCLUSIONS

In this study, the critical issue of the retrofitting of AM buildings has been experimentally investigated. Specifically, the efficiency of two TRM systems made of glass- and hemp-fibre meshes, respectively (both embedded in mud-mortar matrix) was assessed by means of diagonal compression tests on AM wallets. Overall, twenty-one specimens were tested and were equally divided into three groups: unreinforced specimens (URM), specimens strengthened with glass-based TRM (GTRM), and specimens strengthened with hemp-based TRM (HTRM).

Experimental shear stress-strain curves derived according to the ASTM E519-15 standard [29] and observed failure modes allow the following conclusions to be drawn:

- URM specimens failed in diagonal tension with wide cracks along joints and blocks, evidencing negligible pre-peak hardening and a quasi-brittle post-peak behaviour.
- The GTRM strengthening system considerably improved the mechanical behaviour of AM wallets, producing significant hardening until peak stress was reached and post-peak softening. Nevertheless, the failure mode was generally detected by the debonding of the reinforcing glass-fibre grid from the mud-mortar matrix, which limited the ductility capacity. Resulting strength increase with respect to as-built configuration was equal to 10%, on average, whereas the improved ductility was twice.
- Neither debonding nor local failure of the hemp-matrix system was observed on HTRM-strengthened specimens. Their shear behaviour was generally characterized by large hardening after cracking onset and very gradual softening in the post-peak response. Indeed, the observed diagonal cracks gradually developed until failure, the latter being caused by tensile fracture of hemp grid. Accordingly, the HTRM system ensured high efficiency, increasing the unreinforced shear strength by about 30% and resulting into a ductility capacity 3.6 times that of URM wallets.

Definitely, the feasibility of using TRM with the aim to obtain a crucial reduction of the seismic vulnerability of existing AM structures has been illustrated in this study. Both the considered TRM strengthening systems ensured considerable retrofitting efficiency with highly improved energy dissipation of AM wallets. The HTRM solution proved to be preferable due to its major mechanical compatibility with poor mud mortar and adobe blocks. Nevertheless, due to large dispersion of mechanical properties and response, great emphasis should be given on the improvement of the manufacturing process.

REFERENCES

[1] H. Houben, H. Guillaud, *Earth construction — A comprehensive guide*. London: Intermediate Technology Publication, 1994.

[2] B. Briseghella, V. Colasanti, L. Fenu, C. Nuti, E. Spacone, H. Varum, Seismic analysis by macroelements of Fujian Hakka Tulous, Chinese circular earth constructions listed in the UNESCO World Heritage List. *International Journal of Architectural Heritage*, **14**(10), 1551-1566, 2020.

[3] E.L. Tolles, E.E. Kimbro, W.S. Ginell, *Planning and engineering guidelines for the seismic retrofitting of historic adobe structures*. Los Angeles: Getty Publications, 2003.

[4] M. Blondet, G.V. Garcia, S. Brzev, A. Rubiños, *Earthquake-resistant construction of adobe buildings: A tutorial*. EERI/IAEE World Housing Encyclopedia, 2003.

[5] R. Meli, O. Hernandez, M. Padilla, Strengthening of adobe houses for seismic actions. In: *Proceedings of the Seventh World Conference on Earthquake Engineering*, Istanbul, 1980; Vol. 4, p. 465-472.

[6] F. Parisi, N. Augenti, Earthquake damages to cultural heritage constructions and simplified assessment of artworks. *Engineering Failure Analysis*, **34**, 735-760, 2013.

[7] M. Blondet, J. Vargas, J. Velasquez, N. Tarque, Experimental study of synthetic mesh reinforcement of historical adobe buildings. In: *Proceedings of International Conference on Structural Analysis of Historical Constructions*, 2006; p. 715-722.

[8] D. Torrealva, Seismic Design Criteria for Adobe Buildings Reinforced with Geogrids. In: *Proceedings of 15th World Conference on Earthquake Engineering*, Lisboa, 2012.

[9] S. Bossio, M. Blondet, S Rihal, Seismic behavior and shaking direction influence on adobe wall structures reinforced with geogrid. *Earthquake Spectra,* **29**(1), 59-84, 2013.

[10] N. Sathiparan, K. Sakurai, M. Numada, K. Meguro, Seismic evaluation of earthquake resistance and retrofitting measures for two story masonry houses. *Bulletin of Earthquake Engineering*, **12**(4), 1805-1826, 2014.

[11] E.L. Tolles, E.E. Kimbro, F.A. Webster, W.S. Ginell, *Seismic stabilization of historic adobe structures: Final report of the Getty seismic adobe project*. Los Angeles: Getty Publications, 2000.

[12] A. Turer, S.Z. Korkmaz, H.H. Korkmaz, Performance improvement studies of masonry houses using elastic post-tensioning straps. *Earthquake Engineering & Structural Dynamics*; **36**(5), 683-705, 2007.

[13] A. Charleson. *Seismic strengthening of earthen houses using straps cut from used car tires: a construction guide*. Oakland: Earthquake Engineering Research Institute (EERI), 2010.

[14] D.M. Dowling, B. Samali, Low-cost and low-tech reinforcement systems for improved earthquake resistance of mud brick buildings. In: *Proceedings of the Getty seismic adobe project 2006 colloquium*, Los Angeles, 2006.

[15] M. Blondet, J. Vargas-Neumann, R. Groenenberg, Evaluation of the efficacy of mud injection to repair seismic cracks on adobe structures via full-scale shaking table tests. In: *Proceedings of 15th World Conference on Earthquake Engineering*, Lisboa, 2012.

[16] M. Blondet, J. Vargas, C. Sosa, J. Soto, Using mud injection and an external rope mesh to reinforce historical earthen buildings located in seismic areas. In: *Proceedings of 9th International Conference on Structural Analysis of Historical Constructions*, Mexico City, 2014. p 14-17.

[17] C. Oliveira, H. Varum, A. Figueiredo, D. Silveira, A. Costa, Experimental tests for seismic assessment and strengthening of adobe structures. In: *Proceedings of the 14th European conference on earthquake engineering*, Ohrid, 2010.

[18] A. Figueiredo, H. Varum, A. Costa, D. Silveira, C. Oliveira, Seismic retrofitting solution of an adobe masonry wall. *Materials and Structures,* **46**(1-2), 203-219, 2013.

[19] L. Turanli, A. Saritas, Strengthening the structural behavior of adobe walls through the use of plaster reinforcement mesh. *Construction and Building Materials*, **25**(4), 1747-1752, 2011.

[20] C. Atzeni, Stone masonry in rural Sardinian building. Evolution of the traditional building techniques between XIX and XX century. In: *Proceedings of the First International Congress on Construction History*, Madrid, 2003. p. 279-289.

[21] F. Parisi, D. Asprone, L. Fenu, A. Prota, Experimental characterization of Italian composite adobe bricks reinforced with straw fibers. *Composite Structures,* **122**, 300-307, 2015.

[22] D. Asprone, V. Colasanti, L. Fenu, F. Parisi, A. Prota, Adobe in Sardinia. Static and dynamic behaviour of the earthen material and of adobe constructions. In: *Proceedings of the 16th International Brick and Block Masonry Conference*, Padova, 2016.

[23] A. Caporale, F. Parisi, D. Asprone, R. Luciano, A. Prota, Critical surfaces for adobe masonry: micromechanical approach. *Composites Part B: Engineering*, **56**, 790-796, 2014.

[24] A. Caporale, F. Parisi, D. Asprone, R. Luciano, A. Prota, Comparative micromechanical assessment of adobe and clay brick masonry assemblages based on experimental data sets. *Composite Structures*, **120**, 208-220, 2014.

[25] EN 1998–3, *Eurocode 8: design of structures for earthquake resistance – part 3: assessment and retrofitting of buildings*. Brussels: Comité Européen de Normalisation; 2005.

[26] FEMA 356, *Prestandard and commentary for the seismic rehabilitation of buildings*. Washington (DC): Federal Emergency Management Agency; 2000.

[27] Italian Building Code Commentary, Circolare n. 617 del 02.02.2009: *Istruzioni per l'applicazione delle «Nuove Norme Tecniche per le Costruzioni» di cui al decreto ministeriale 14 gennaio 2008*. Rome: Italian Ministry of Infrastructures and, Transportation; 2009 [in Italian].

[28] C. Menna, D. Asprone, M. Durante, A. Zinno, A. Balsamo, A. Prota, Structural behaviour of masonry panels strengthened with an innovative hemp fibre composite grid. *Construction and Building Materials*, **100**, 111-121, 2015.

[29] ASTM E 519-15 – *Standard test method for diagonal tension (shear) in masonry assemblages*. ASTM International, West Conshohocken, PA, USA, 2015.

[30] A. Bonati, A. Franco, O. Coppola, G. De Luca, Strengthening of masonry structures: Current national and international approaches for qualification and design. *Key Engineering Materials* **817**, 501-506, 2019.